Packet-Reduced Ranging Method with Superresolution TOA Estimation Algorithm for Chirp-Based RTLS

Daegun Oh, Seungryeol Go, and Jong-wha Chong

In this paper, a packet-reduced ranging method using a superresolution time of arrival estimation algorithm for a chirp-based real-time locating system is presented. A variety of ranging methods, such as symmetric double-sided two-way ranging (SDS-TWR), have been proposed to remove the time drift due to the frequency offset using extra ranging packets. Our proposed method can perform robust ranging against the frequency offset using only two ranging packets while maintaining almost the same ranging accuracy as them. To verify the effectiveness of our proposed algorithm, the error performance of our proposed ranging method is analyzed and compared with others. The total ranging performance of TWR, SDS-TWR, and our proposed TWR are analyzed and verified through simulations in additive white Gaussian noise and multipath channels in the presence of the frequency offset.

Keywords: TOA, chirp spread spectrum, RTLS, SDS-TWR, ranging packet.

Manuscript received Oct. 5, 2012; revised Jan. 8, 2013; accepted Jan. 9, 2013.

This work was supported by the IT R&D program of MKE/KEIT [10035570, Development of self-powered smart sensor node platform for Smart&Green building]. This work was supported by the DGIST R&D Program of the Ministry of Education, Science and Technology of Korea (13-RS-02). This research was supported by the Ministry of Knowledge Economy (MKE), Korea, under the Information Technology Research Center (ITRC) support program supervised by the National IT Industry Promotion Agency (NIPA) (NIPA-2013-H0301-13-1011).

Daegun Oh (phone: +82 53 785 4583, dgoh@dgist.ac.kr) was with the Department of Electronics and Computer Engineering, Hanyang University, Seoul, Rep. of Korea, and is now with Daegu Gyeongbobk Institute of Science & Technology (DGIST), Daegu, Rep. of Korea.

Seungryeol Go (corresponding author, milkyface@hanyang.ac.kr) and Jong-wha Chong (jchong@hanyang.ac.kr) are with the Department of Electronics and Computer Engineering, Hanyang University, Seoul, Rep. of Korea.

http://dx.doi.org/10.4218/etrij.13.0112.0678

I. Introduction

Real-time locating systems (RTLSs) are proving increasingly useful in the sensor network area to meet the increasing demand for such location services as asset tracking, finding people on the move, and mobile tracking in emergency situations in which a GPS receiver is impractical.

Recently, chirp spread spectrum (CSS) was adopted as the ISM band baseline standard of IEEE 802.15.4a [1] as well as the ISO/IEC 24730-5 [2], organized for the development of an RTLS with high accuracy. In this paper, accordingly, chirp signals are assumed to be baseband signals of a ranging packet. The ranging scheme is classified as a synchronous (one-way) or an asynchronous (two-way) ranging system whether or not it uses a global synchronization. Recently, the asynchronous two-way ranging (ATWR) scheme caught on commercially since it does not require both the global synchronization and expensive oscillators. In the ATWR system, the time of flight (TOF) is used to estimate the distance between two nodes. We can extract TOF information from the estimated round-trip time (RTT) with the knowledge of the reply time.

In estimating the RTT, a ranging error occurs due to the frequency offset between two nodes. In the literature, a variety of the modified TWR protocols, such as symmetric double-sided TWR (SDS-TWR) [3], asymmetric double-sided TWR (ADS-TWR) [4], double-TWR [5], and SDS-TWR with multiple acknowledgement (SDS-TWR-MA) [6], were proposed to eliminate the ranging error caused by frequency offset. For these protocols [3]-[6] developed against frequency offset, more than three ranging packets are required to make a pair of RTTs for cancellation of the ranging error. This forces mobile nodes to consume more battery power, which results in short battery life. Since a mobile node has a finite battery

capacity, power saving is one of the most critical issues.

The other critical issue is ranging accuracy mostly depending on bandwidth, signal-to-noise ratio (SNR), observation time, and so on, as in [7]. In indoor surroundings, a direct path containing range information is superimposed with many reflected paths. Without enough bandwidth, it is hard to detect the time of arrival (TOA) of the direct path correctly due to superimposed paths. To resolve this kind of TOA estimation problem of the narrowband signals, MUSIC-based superresolution (SR) algorithms [8], [9] have been proposed with channel frequency estimation (CFR) preprocessing because of its superior decomposing ability in a line-of-sight multipath environment. However, CFR estimation requires a discrete Fourier transform (DFT) [10], and the MUSIC algorithm needs such matrix decompositions as eigenvalue decomposition (EVD) and singular value decomposition (SVD). Although TOA estimation using the decompositions is preferred for its superior performance, the decompositions are difficult to implement in a hardware system without loss of accuracy.

In this paper, we suggest a new packet-reduced ranging protocol with a low complexity SR TOA estimation algorithm to implement a low power consuming RTLS. Although our proposed protocol is based on only two ranging packets, it can achieve almost the same error performance as SDS-TWR using more than three ranging packets. In the case of SDS-TWR, it tries to resolve the problem of performance degradation due to the frequency offset by the RTT averaging scheme, which requires more than three ranging packets. However, using our proposed method, a low power consuming ranging system can be achieved with two ranging packets without performance degradation. The propagator method (PM) [11], one of the SR techniques used for optimal beamforming, is known to have a low complexity since it does not require such matrix decompositions as SVD and EVD. However, it is not directly applicable to the TOA estimation problem of a chirp-based RTLS. Thus, the PM is modified and combined with our proposed packet-reduced ranging method for a low complexity RTLS realization. Finally, in a given SNR and bandwidth, the total ranging errors, composed of the TOA estimation error and RTT estimation error, are analyzed for each of the following: TWR, SDS-TWR, and our proposed method. We verify that the analyzed results are consistent with the simulation results.

II. Signal Model

In this section, a chirp-based ranging packet perturbed by the frequency offset is modeled, and our proposed ranging protocol is then derived based on the signal model.

A transmitted ranging packet is assumed to be composed of a training and data sequence in accordance with the relevant baseline standards in [1], [2], as shown in Fig. 1. For initial acquisition of the ranging packet, the received symbols in the training sequence composed of preamble and start frame delimiter (SFD) are used for gain control, packet detection, frame synchronization, and frequency synchronization. Without loss of generality, we assume that these preliminary steps have been done successfully and focus on explaining the main idea behind our proposed TWR algorithm. After frequency synchronization using preamble signals as in [12], [13], the carrier frequency offset (CFO) can be almost completely removed but the sampling frequency offset (SFO) remains. Consider the baseband chirp symbol

$$s(t)=\begin{cases}\exp\left[j\left(\omega_s t+\frac{\mu}{2}t^2\right)\right] & \text{for } 0\le t<T_{\text{sym}},\\ 0 & \text{elsewhere,}\end{cases} \quad (1)$$

where ω_s is the start frequency of the chirp signal and μ is the rate of change of the instantaneous frequency as modeled in [1], [2]. The received M symbols perturbed by a multipath channel and additive white Gaussian noise (AWGN) can be modeled by

$$y(t)=\left[\sum_{k=0}^{M-1}\sum_{m=1}^{d}\exp\left(jb_k\right)a_m s\left(t-kT_{\text{sym}}-\tau_m\right)\right]+w(t), \quad (2)$$

where $w(t)$ is the AWGN and T_{sym} is the symbol period. The complex amplitude and TOA of the m-th path are a_m and τ_m, respectively. The modulated phase of the k-th symbol is b_k. The number of symbols of a ranging packet is M. The number of paths is d. For a given frequency offset of Node A and Node B, denoted by β_A and β_B, respectively, in parts per million, the time drift over the sampling period T_s and symbol period T_{sym} can be represented by

$$O_s=T_s\varepsilon_A \text{ and } O_y=T_{\text{sym}}\varepsilon_A, \quad (3)$$

where

$$\varepsilon_A=\frac{-\beta_A}{1+\beta_A} \text{ and } \varepsilon_B=\frac{-\beta_B}{1+\beta_B}. \quad (4)$$

The parameters ε_A and ε_B were also used in [14] to express the sampling and symbol delay due to the sampling frequency offset. Define $y_l^A(n)$ as the n-th received sample of the l-th chirp symbol at Node A and $y_l^B(n)$ as the n-th received sample of the l-th chirp symbol at Node B. Using (3) and (4), they can be expressed in terms of the relative frequency offsets $\beta_{AB}=\beta_A-\beta_B$ and $\beta_{BA}=\beta_B-\beta_A$ by

$$y_l^A(n)=\left(\sum_{m=1}^{d}a_m s\left(n\left(T_s+O_s^{BA}\right)+lO_y^{BA}+\tau_m\right)\right) \text{ for } n=0,1,\ldots,N-1, \quad (5)$$

$$y_l^{\mathrm{B}}(n)=\left(\sum_{m=1}^{d} a_m s\left(n\left(T_{\mathrm{s}}+O_{\mathrm{s}}^{\mathrm{AB}}\right)+lO_{\mathrm{y}}^{\mathrm{AB}}+\tau_m\right)\right) \text{ for } n=0,\ 1,\ldots,\ N-1, \tag{6}$$

where

$$O_{\mathrm{s}}^{\mathrm{AB}}=T_{\mathrm{s}}\varepsilon_{\mathrm{AB}},\ O_{\mathrm{y}}^{\mathrm{AB}}=T_{\mathrm{sym}}\varepsilon_{\mathrm{AB}},\ O_{\mathrm{s}}^{\mathrm{BA}}=T_{\mathrm{s}}\varepsilon_{\mathrm{BA}},\ O_{\mathrm{y}}^{\mathrm{BA}}=T_{\mathrm{sym}}\varepsilon_{\mathrm{BA}}, \tag{7}$$

$$\varepsilon_{\mathrm{AB}}=\frac{-\beta_{\mathrm{AB}}}{1+\beta_{\mathrm{AB}}} \text{ and } \varepsilon_{\mathrm{BA}}=\frac{-\beta_{\mathrm{BA}}}{1+\beta_{\mathrm{BA}}}. \tag{8}$$

In (5) and (6), N is the number of samples of a symbol, that is, $T_{\mathrm{sym}}=NT_{\mathrm{s}}$.

III. Ranging Protocol

The ATWR estimates the distance between two nodes by calculating the TOF. In this section, we illustrate how our proposed protocol removes the induced ranging error due to the frequency offset as compared with the conventional algorithms, such as TWR and SDS-TWR. In general, in calculating the TOF, it is essential to estimate the TOA of the direct path. Assuming there is no frequency offset, a ranging error arises due to noise and self-interference in estimating the TOA of the direct path. In the next section, the TOA estimation error is considered and combined with the ranging error due to the frequency offset.

1. TWR

The TWR protocol [15] is the simplest among the ranging protocols, and it can calculate the distance of two nodes by using only two packets.

Figure 1 shows the procedure of the conventional TWR in a two-node scenario. As illustrated in Fig. 1, the TOF is calculated by

$$t_{\mathrm{p}}=\frac{1}{2}\left(t_{\mathrm{round}}-T_{\mathrm{replyB}}\right), \tag{9}$$

where t_{round} represents the RTT at Node A and t_{p} is the TOF. The reply time of Node B is denoted by T_{replyB} and is the delay between the end of a received packet and the beginning of the next transmission at Node B. However, this protocol has a serious ranging error due to not taking the frequency offset into account. In a given frequency offset, β_{A} and β_{B}, the ranging error can be formulated using some derivations in [15] by

$$e_{\mathrm{TWR}}=t_{\mathrm{p}}\varepsilon_{\mathrm{A}}+\frac{1}{2}\varepsilon_{\mathrm{A}}T_{\mathrm{replyB}}\left(1+\varepsilon_{\mathrm{B}}\right). \tag{10}$$

From (10), it is noteworthy that the ranging error is affected by the reply time T_{replyB}, which is quite large. The first term in (10) is negligible, but the second term produces a large ranging error.

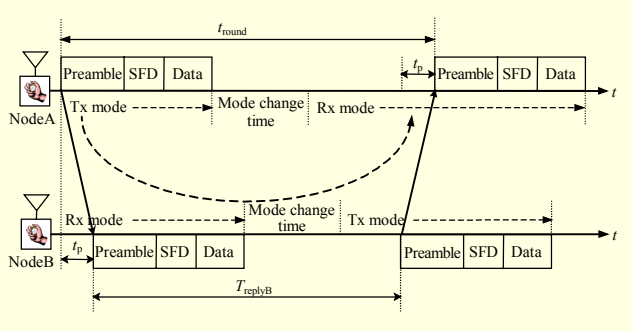

Fig. 1. Conventional TWR protocol.

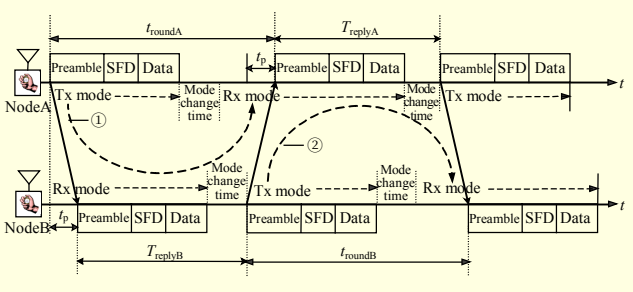

Fig. 2. Conventional SDS-TWR protocol.

2. SDS-TWR

The SDS-TWR protocol [3] is proposed to reduce the ranging error of TWR. It is impossible to remove the error completely, but the second term of (10) can be almost completely removed by SDS-TWR. For SDS-TWR to work properly, more than four packets are required with the assumption that $T_{\mathrm{replyA}}= T_{\mathrm{replyB}}$, as in [3].

Figure 2 shows the entire process of the SDS-TWR. We can see that two RTTs, denoted by t_{roundA} and t_{roundB}, are estimated using the paths ① and ②, respectively. The paths ① and ② share the second TOF, as in Fig. 2. This is the reason SDS-TWR can make two RTTs using only three ranging packets. These two RTTs are respectively defined as

$$t_{\mathrm{roundA}} = 2t_{\mathrm{p}}+T_{\mathrm{replyB}} \tag{11}$$

and

$$t_{\mathrm{roundB}} = 2t_{\mathrm{p}}+T_{\mathrm{replyA}}. \tag{12}$$

Due to the sampling frequency offset, the reply times T_{replyA} and T_{replyB} are counted incorrectly at Node A and Node B. By averaging two RTTs t_{roundA} and t_{roundB}, we can eliminate the offset-induced ranging error. Referring to [16], the ranging

error of SDS-TWR is derived by

$$e_{\text{SDS-TWR}} = \frac{1}{2} t_{\text{p}} \left(\varepsilon_{\text{A}} + \varepsilon_{\text{B}} \right) + \frac{1}{4} \left(\left(T_{\text{replyB}} - T_{\text{replyA}} \right) \left(\varepsilon_{\text{B}} - \varepsilon_{\text{A}} \right) \right). \quad (13)$$

Using the assumption of $T_{\text{replyA}}=T_{\text{replyB}}$, $e_{\text{SDS-TWR}}$ is approximated as

$$e_{\text{SDS-TWR}} \approx \frac{1}{2} t_{\text{p}} \left(\varepsilon_{\text{A}} + \varepsilon_{\text{B}} \right). \quad (14)$$

3. Proposed TWR Protocol

After SDS-TWR [3] was proposed, its variations, such as SDS-TWR-MA [6], double-TWR [5], and so on, emerged for robust ranging against a frequency offset. Most of these are based on the approach of RTT averaging, illustrated in Fig. 2. Thus, they also need more than three ranging packets, as with SDS-TWR. Compared with TWR, they provide more accurate ranging performances. At the same time, however, the battery life is shortened as the number of transmitted ranging packets increases [6].

Our proposed algorithm can achieve almost the same accuracy as SDS-TWR and its variations [3]-[6] using only two ranging packets. Instead, the additional signal processing is needed for our proposed algorithm to work properly.

The main idea behind our proposed algorithm is to make a pair of RTT paths, reflective of the construct in SDS-TWR. In the case of SDS-TWR, a pair of RTT paths is made by using more than three ranging packets, as shown in Fig. 2. However, our proposed algorithm makes a pair of RTT paths: One path, denoted by ① in Fig. 3, estimates the RTT from the beginning of the ranging packet; The second path, denoted by ②, estimates the RTT from the end of the ranging packet.

From path ①, RTT $t_{\text{round,A1}}$ can be estimated. Likewise, RTT $t_{\text{round,A2}}$ is estimated from path ②. $T_{\text{pac,A}}$ and $T_{\text{pac,B}}$ denote the duration of the packet transmitted by local frequency of Node A and Node B, respectively. The reply time by SDS-TWR at Node A, denoted by T_{replyA}, is generally assumed to be the same as the reply time by SDS-TWR at Node B, denoted by T_{replyB}, that is, $T_{\text{replyA}}=T_{\text{replyB}}$. However, the reply times of our proposed algorithm, denoted by T_{replyB1} and T_{replyB2}, are given differently as

$$T_{\text{replyB1}} = T_{\text{pac,A}} + \hat{T}_{\text{pac,A}} \quad (15)$$

and

$$T_{\text{replyB2}} = \hat{T}_{\text{pac,A}}, \quad (16)$$

where $\hat{T}_{\text{pac,A}}$ is the estimate of $T_{\text{pac,A}}$ at Node B. After the recognition of the received packet at Node B, the sampling delay is accumulated until the end of the ranging packet, resulting in time difference e_{s}, as shown in Fig. 3. If we can

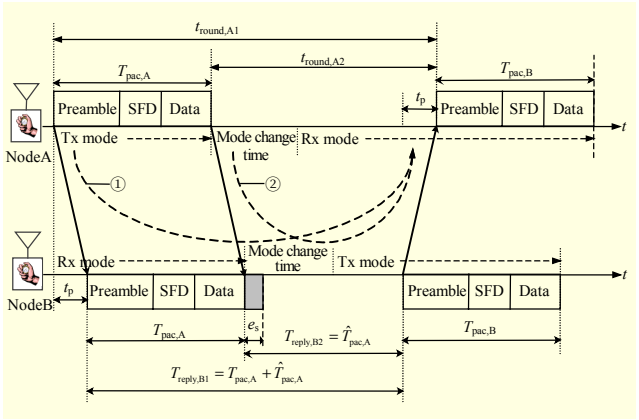

Fig. 3. Proposed TWR protocol.

estimate e_{s} correctly, we can know $T_{\text{pac,A}}$ by

$$\hat{T}_{\text{pac,A}} = T_{\text{pac,B}} - \hat{e}_{\text{s}} \text{ with } \hat{e}_{\text{s}} = e_{\text{s}} + \eta_{\text{pac}}. \quad (17)$$

The estimation of e_{s} is addressed in the next section. Assuming $\hat{T}_{\text{pac,A}}$ is perfectly estimated at Node B, the RTTs for ① and ② are modeled by

$$t_{\text{round,A1}} = 2t_{\text{P}} + T_{\text{replyB1}} = 2t_{\text{P}} + T_{\text{pac,A}} + \hat{T}_{\text{pac,A}} \quad (18)$$

and

$$t_{\text{round,A2}} = 2t_{\text{P}} + T_{\text{replyB2}} = 2t_{\text{P}} + \hat{T}_{\text{pac,A}}. \quad (19)$$

In the case of SDS-TWR and its variations, two RTTs are counted by Node A and Node B, respectively, and both of them are then averaged to reduce the ranging error. In contrast, two RTTs are counted by the local frequency of Node A for our proposed TWR algorithm, as shown in Fig. 3. Therefore, we cannot avoid the time drift by the sampling frequency offset over $t_{\text{round,A1}}$ or $t_{\text{round,A2}}$. However, since the reply times are given in terms of $\hat{T}_{\text{pac,A}}$, as in (18) and (19), respectively, it can be easily seen that T_{replyB1} is exactly twice that of the T_{replyB2} with an assumption of no estimation error of $\hat{T}_{\text{pac,A}}$. Exploiting this relation, we can remove the induced time drift in $t_{\text{round,A1}}$ or $t_{\text{round,A2}}$ as follows:

$$t_{\text{P}} = t_{\text{round,A2}} - \frac{t_{\text{round,A1}}}{2}. \quad (20)$$

In this way, the time drift over the reply times can be removed but the time drift over the propagation times remains. Thus, the ranging error due to frequency offset for our proposed algorithm is represented by

$$e_{\text{prop.TWR}} = t_{\text{p}} \varepsilon_{\text{A}}. \quad (21)$$

4. Comparison

We compare our proposed algorithm with the conventional

Table 1. Comparison of ranging protocols.

	TWR	SDS-TWR	Proposed TWR
Required ranging packets	2	3	2
Required data packets	0	1	0
Number of TOA est.	2	3	2
Number of RTT est.	1	2	2
Ranging error	$e_{TWR} >> e_{SDS\text{-}TWR} \approx e_{prop.twr}$		
Necessity for offset est.	no need	no need	need

algorithms regarding various aspects, including the required data packets, the required number of TOA estimations, and the ranging errors. The results are summarized in Table 1.

As shown in Table 1, the SDS-TWR protocol makes use of a total of four packets to measure the distance between two nodes, respectively. However, our proposed TWR protocol requires only two packets while maintaining almost the same ranging performance as SDS-TWR. Since the number of packets used in SDS-TWR is reduced by half in our proposed ranging protocol while retaining ranging performance, our proposed algorithm can be regarded as effective in terms of power consumption and packet utilization.

IV. TOA and $T_{pac,A}$ Estimation

Time-based ranging methods [17], [18] are all in need of TOA estimation of the direct path since the direct path involves distance information. There are two approaches to estimate the TOA of the direct path. One is based on maximum likelihood estimation [19], [20], and the other is based on SR algorithms [21], [22]. In the case of narrowband signals, the SR algorithms are preferred for their superior decomposing capability for the received superimposed signals.

Almost all SR algorithms are based on the superiority of SVD and EVD in extracting the phase shift, caused by the TOA of the direct path. However, such decompositions as SVD and EVD increase the complexity on ranging system. Therefore, we consider a low cost SR algorithm that does not use decompositions, referred to as the PM. The algorithm has been combined with our proposed preprocessing method to estimate the TOA of the direct path and e_s for the received ranging packet composed of chirp symbols.

1. Estimation of $T_{pac,A}$ at Node B

For our proposed ranging protocol to work properly, it is essential to estimate the $T_{pac,A}$ correctly. By the following two methods, we can estimate the time drift e_s in (17).

A. Estimation Based on Single Set

In (6), the received chirp samples at Node B are modeled with symbol delay O_y^{AB} and sample delay O_s^{AB}. Since the sample delay within a symbol is negligible, that is, $O_y^{AB} >> O_s^{AB}$, we only consider the symbol delay hereafter. Before we apply the PM, we must transform the received chirp signals into the sinusoid. By doing so, the symbol delay O_y^{AB} can be changed to the frequency parameter of the sinusoid. Assuming the received two symbols, p-th and q-th, satisfy $p > q$, the transformed sinusoid can be defined by

$$f(n) \approx y_p^B(n) \times \left(y_q^B(n)\right)^* \text{ for } n=0, 1,..., N-1. \quad (22)$$

This is basically the same kind of transformation used for TOA estimation in (27) and (28), called dechirping. Dechirping converts the received chirp signals into the sum of sinusoids by multiplying them by the reference chirp signal, as in (27). However, in (22), the reference signal is also the received q-th chirp symbol. As in (28), the multiplication of (22) produces a variety of sinusoids, but the dominant one is

$$f(n) = \exp(j\kappa n T_s) \text{ where } \kappa = \mu O_y^{BA}(p-q). \quad (23)$$

The frequency of the approximated sinusoid is κ, linearly proportional to the symbol delay between the p-th and the q-th symbol. Every path of the received symbol of q-th is delayed by $(p-q)O_y^{BA}$ from the p-th received symbol due to sampling the frequency offset. Thus, the sinusoid of $f(n)$ is averaged for all M paths. We can estimate the frequency of $f(n)$ by using the PM. Assuming that the frequency estimate $\hat{\kappa}$ of $f(n)$ is given by the PM, e_s can be derived from $\hat{\kappa}$ by

$$\hat{e}_s = \frac{MT_s}{\mu(p-q)}\hat{\kappa}. \quad (24)$$

B. Estimation Based on Multiple Sets

The above estimation is based on a pair of two symbols. Multiple sets are possibly applicable for accuracy enhancement. Basically, the estimation approach is the same as in (22) through (24). Since the assumed p-th and q-th symbols are selectable among all M symbols satisfying $p > q$, R sets are made by

$$\left[\left\{y_r^B, y_{p-q+r}^B\right\}\right]_{r=0}^{R-1}. \quad (25)$$

2. TOA Estimation of Direct Path

For our proposed TWR protocol, the TOA estimation of the direct path should be executed two times at Node A and Node B, respectively. Since the algorithm runs in the same way regardless of the nodes, we only consider the TOA estimation

for the l-th symbol of the received signals at Node B, $y_l^{\mathrm{B}}(n)$.

We model each of the received paths with respect to t=0 as

$$y_l^{\mathrm{B}}(n) \approx \left(\sum_{m=1}^{d} a_m s\left(nT_{\mathrm{s}} - \tau_m\right) \right). \quad (26)$$

In this section, we have not considered sampling delay $O_{\mathrm{s}}^{\mathrm{AB}}$ within the l-th symbol since it is generally very small (under 1 ns).

Prior to the TOA estimation by SR algorithms, we must transform the received signals into a form of sinusoid [10]. Conventional SR algorithms [21], [22] transform each of the received signals into the form of the corresponding sinusoid by using DFT and deconvolution, that is, CFR estimation. However, chirp signals can be changed to the sinusoids by a dechirping process:

$$d(n) = y_l^{\mathrm{B}}(n) \times s^*(t), \quad (27)$$

where $d(n)$ represents the transformed samples, and it can be rewritten as

$$d(n) = \left(\sum_{m=0}^{M-1} a_m \exp\left[j\left(\underbrace{-\mu\tau_m}_{\text{frequency}} T_{\mathrm{s}} n - \omega_{\mathrm{s}}\tau_m + \frac{\mu}{2}\tau_m^{\,2} \right) \right] \right). \quad (28)$$

In (28), the transformed signals are composed of the sinusoids that bear a frequency of $-\mu\tau_m$. In this way, the TOA estimation of the received signal $y_l^{\mathrm{B}}(n)$ is changed to the frequency estimation of $d(n)$.

The PM [11] can be summarized as follows. The smoothed matrix $\mathbf{D}$ comprises elements of $d(n)$ as follows:

$$\mathbf{D} = \begin{bmatrix} d(0) & \cdots & d(L-1) \\ \vdots & \cdots & \vdots \\ d(N-L) & \cdots & d(N-1) \end{bmatrix} \text{ where } L \geq d. \quad (29)$$

The PM makes a pair of submatrices by row extractions from the data matrix as follows:

$$\mathbf{D} = \begin{bmatrix} \mathbf{D}^{(0:d-1)} \\ \mathbf{D}^{(d:N-L)} \end{bmatrix} \begin{matrix} \}d \text{ rows} \\ \}N-L-d \text{ rows} \end{matrix}. \quad (30)$$

$\mathbf{D}^{(x:y)}$ denotes the extracted submatrix from the x-th row to the y-th row from data matrix $\mathbf{D}$. Using $\mathbf{D}^{(0:d-1)}$ and $\mathbf{D}^{(d:N-L)}$, we can describe propagator $\mathbf{P}$, a transformation matrix that satisfies

$$\begin{bmatrix} \mathbf{P}^H & -\mathbf{I}_{d-N} \end{bmatrix} \begin{bmatrix} \mathbf{D}^{(0:d-1)} \\ \mathbf{D}^{(d:N-L)} \end{bmatrix} = \mathbf{0}, \quad (31)$$

where the subscript H denotes the Hermitian operator. $\mathbf{0}$ is the zero matrix and $\mathbf{I}_{d-N}$ is the identity matrix of size $d-N$ by $d-N$. For the estimation of $\mathbf{P}$, least square approximation can be defined as

$$\hat{\mathbf{P}} = \arg\ \min \left\| \mathbf{D}^{(d:N-L)} - \mathbf{P}^H \mathbf{D}^{(0:d-1)} \right\|^2 = \left(\mathbf{D}^{(0:d-1)} \left(\mathbf{D}^{(0:d-1)} \right)^H \right)^{-1} \mathbf{D}^{(0:d-1)} \left(\mathbf{D}^{(d:N-L)} \right)^H. \quad (32)$$

Using the estimation of $\mathbf{P}$, the pseudospectrum can be estimated in the same way of the MUSIC algorithm [8], [9]. By peak detection algorithm, the frequency components of the superimposed sinusoids can be estimated from the pseudospectrum. Among the frequency estimates, the TOA estimate of the direct path can be found by selecting the minimum value and dividing it by μT_{s}.

V. Performance Analysis

In section III, the ranging error was analyzed for TWR, SDS-TWR, and our proposed method in terms of the relevant parameters concerning the frequency offset, as in (10), (14), and (21), respectively. In this section, we additionally derive the root mean square error (RMSE) for the TOA estimation in terms of the used signal parameters. Then, the TOA estimation error is combined with the ranging error, resulting in the total ranging error for TWR, SDS-TWR, and our proposed TWR.

Assuming an AWGN channel, the RMSE of the direct path, denoted by $\sigma(\tilde{\tau}_0)$, can be expressed according to [23] as

$$\sigma(\tilde{\tau}_0) \approx \frac{1}{\rho_\tau} \sqrt{\frac{1}{N^2} \frac{1}{10^{0.1\times(\mathrm{SNR})}}} \text{ where } \rho_\tau = \mu T_{\mathrm{s}}. \quad (33)$$

In (33), SNR denotes the average SNR in dB, and the scale factor ρ_τ is the parameter used for the transformation from the estimate of the phase shift into the TOA estimate of the direct path. Actually, the propagator matrix produces the phase shift between adjacent samples due to the TOA. Thus, the phase shift can be defined by $\mu T_m T_{\mathrm{s}}$, and this is the reason we take the scale factor as in (33) for RMSE of the TOA estimate. From (33), it can be seen that the RMSE is directly proportional to $1/\rho_\tau$, and this means that the more value the scale factor has, the more accuracy we obtain. Similar to that which is featured in (33), the RMSE of the estimate for $T_{\mathrm{pac,A}}$ can be derived by

$$\sigma(\tilde{T}_{\mathrm{pac,A}}) \approx \frac{1}{\rho_{\mathrm{T}}} \sqrt{\frac{1}{N^2} \frac{1}{10^{0.1\times(\mathrm{SNR}-3)}}} \text{ where } \rho_{\mathrm{T}} = \frac{(p-q)\mu}{MT_{\mathrm{s}}}. \quad (34)$$

The scale factor ρ_{T} is determined according to the relation of (22). Comparing (33) with (34), it can be seen that the SNR loss of 3 dB is applied to (34). This is because the multiplication of a pair of the received symbols in (22) degrades the SNR. In the case of the TOA estimation, the received chirp symbol is multiplied with a reference signal, not the received signal, so that there is no SNR reduction in the

RMSE of (33). Combining (33), (34), and (21), the total ranging error can be described as

$$\sigma_{\text{prop}}\left(\tilde{t}_{\text{p}}\right) \approx t_{\text{P}}\varepsilon_{\text{A}} + \sqrt{2}\sigma\left(\tilde{\tau}_0\right) + \sigma\left(\tilde{T}_{\text{pac,A}}\right). \quad (35)$$

In (35), we can see that $\sigma(\hat{\tau}_0)$ is multiplied by $\sqrt{2}$. This is because the TOA estimation is performed twice at Node A and Node B. Comparing ρ_{T} with ρ_{τ}, we can see $\rho_{\text{T}} \gg \rho_{\tau}$ so that $\sigma(\hat{\tau}_0) \ll \sigma(\tilde{T}_{\text{pac,A}})$. Thus, the simplified version of the RMSE can be written as

$$\sigma_{\text{prop}}\left(\tilde{t}_{\text{p}}\right) \approx t_{\text{P}}\varepsilon_{\text{A}} + \sqrt{2}\sigma\left(\tilde{\tau}_0\right). \quad (36)$$

The RMSE for the conventional TWR and SDS-TWR can be derived in a similar way to that which is featured in (36):

$$\sigma_{\text{TWR}}\left(\tilde{t}_{\text{p}}\right) \approx t_{\text{p}}\left(\varepsilon_{\text{A}}\right) + \frac{1}{2}\left(t_{\text{reply}}\left(\varepsilon_{\text{A}}\right)\left(1+\varepsilon_{\text{B}}\right)\right) + \sqrt{2}\sigma\left(\tilde{\tau}_0\right) \quad (37)$$

and

$$\sigma_{\text{SDS-TWR}}\left(\tilde{t}_{\text{p}}\right) \approx \frac{1}{2}t_{\text{P}}\left(\varepsilon_{\text{A}} + \varepsilon_{\text{B}}\right) + \frac{\sqrt{6}}{2}\sigma\left(\tilde{\tau}_0\right). \quad (38)$$

In (38), $\sigma(\hat{\tau}_0)$ is multiplied by $\sqrt{6}/2$ for SDS-TWR. In the case of TWR and our proposed TWR, only two ranging packets are used. However, SDS-TWR permits three ranging packets, and the TOA estimate for the second ranging packet is used twice in calculating the TOF from path ① and path ②, as shown in Fig. 2. Since two estimates of the TOF are averaged finally, we divide $\sqrt{6}$ by 2, resulting in the form of (38).

VI. Simulation Results

In this section, we illustrate the ranging performance of our proposed protocol compared to those of SDS-TWR and TWR in the presence of the frequency offset in the AWGN channel. The noticeable thing is that we have simulated the TOA estimation algorithm for the received ranging packet in calculating the TOF from the estimate of the RTT.

In the following figures, we compare the analyzed results derived in the preceding section with the simulation results to confirm the consistency. The default simulation parameters are as shown in Table 2.

The parameters β_{A} and β_{B}, denoting the frequency offset of Node A and Node B, respectively, are not included in Table 2 since they are varied in each figure. All of the experimental RMSEs of the estimates are based on 1e6 Monte Carlo runs. Figures 4 and 5 show the experimental RMSEs of the estimate of the TOF as a function of the offset of Node B and Node A, respectively. The other parameters except the frequency offsets are fixed, as shown in Table 2.

In Fig. 4, the RMSEs for the protocols are not varied to the frequency offset of Node A. In the case of SDS-TWR and our proposed TWR, the ranging error due to the frequency offset is considerably small as compared to the TOA estimation error caused by AWGN. That is the reason the RMSEs of SDS-TWR and our proposed TWR seem to be saturated regardless of the frequency offset. In the case of TWR, we can see that the frequency offset of Node B negligibly affects the RMSE from (35). Thus, although the RMSE of TWR is fixed irrespective of the frequency offset of Node B, as shown in Fig. 4, we can see that it is changed according to the frequency offset of Node A, as shown in Fig. 5. This can be explained by (35), in which the offset parameter of Node B is multiplied by that of Node A and t_{reply}. For the offset parameter of Node A, it is multiplied by t_{reply}.

From all of the figures wherein TWR, SDS-TWR, and our proposed TWR are simulated, the RMSE of SDS-TWR is shown to be the lowest among them. This results from the utilization of three ranging packets, leading to more TOA estimates that can be used for averaging. We have already taken this into account in the analysis of (36).

In Figs. 6 through 8, RMSEs are given as a function of the SNR for the given frequency offset of Node A and Node B. When there is no frequency offset, the RMSE is affected by the

Table 2. Simulation parameters.

Parameter	Value	Parameter	Value	Parameter	Value
ω_{s}	0	μ	4.6e+13	T_{sym}	1.1875e–6
T_{s}	3.125e–8	M	100	p	20
q	70	N	38	t_{p}	1e–7
T_{replyA}	3e–4	T_{replyB}	3e–4		

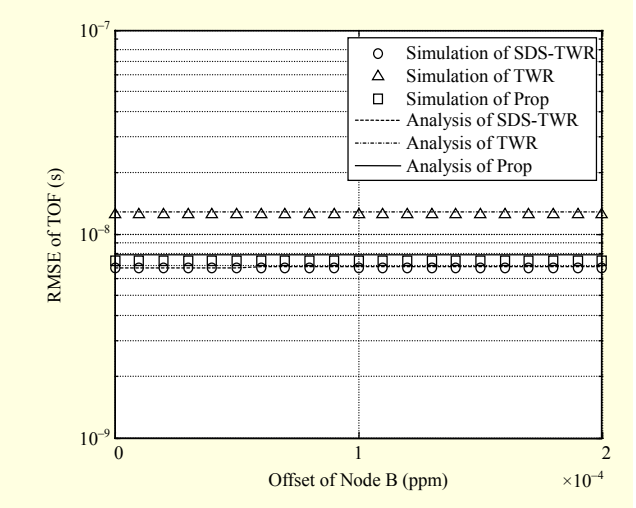

Fig. 4. Performance comparison of relative offsets (frequency offset of Node A = 10 ppm; SNR = 25 dB).

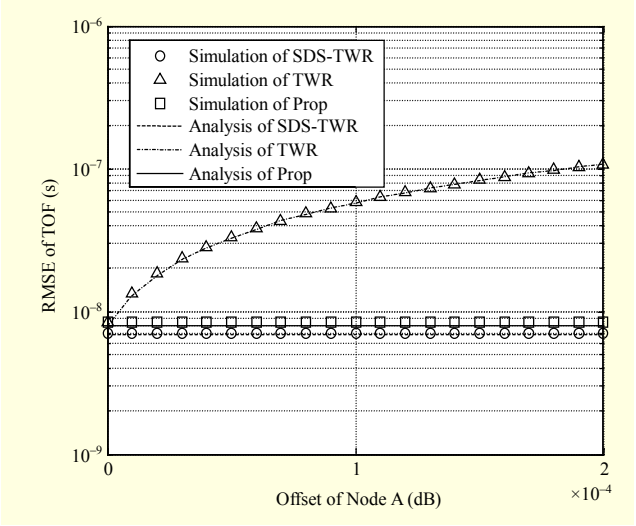

Fig. 5. Performance comparison of relative offsets (frequency offset of Node B = 10 ppm; SNR = 25 dB).

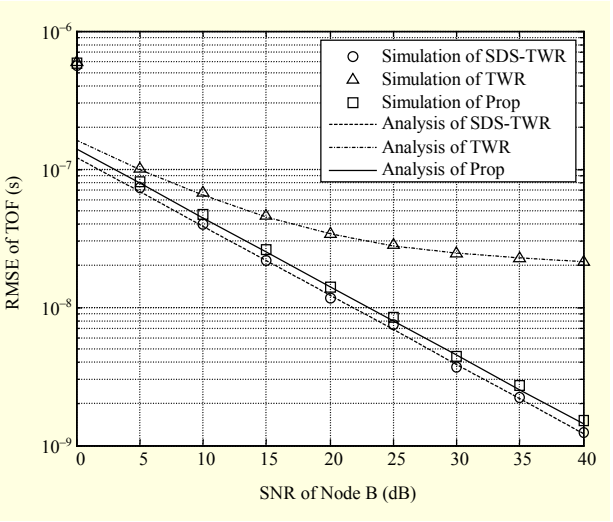

Fig. 7. Ranging performance of each protocol (frequency offset of Node A = 40 ppm; frequency offset of Node B = –40 ppm).

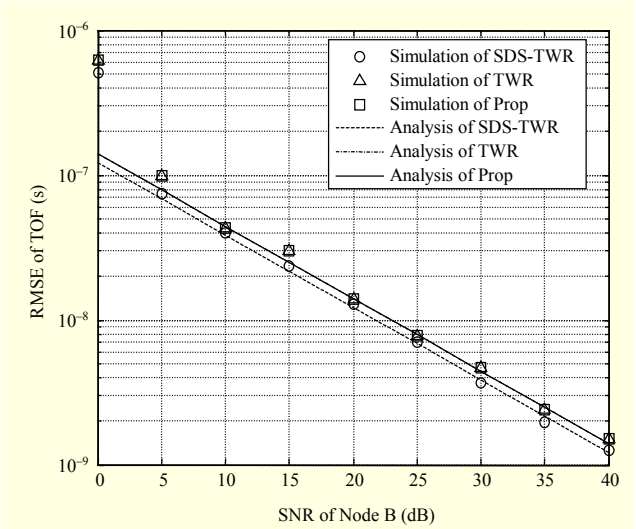

Fig. 6. Ranging performance of each protocol (no frequency offset).

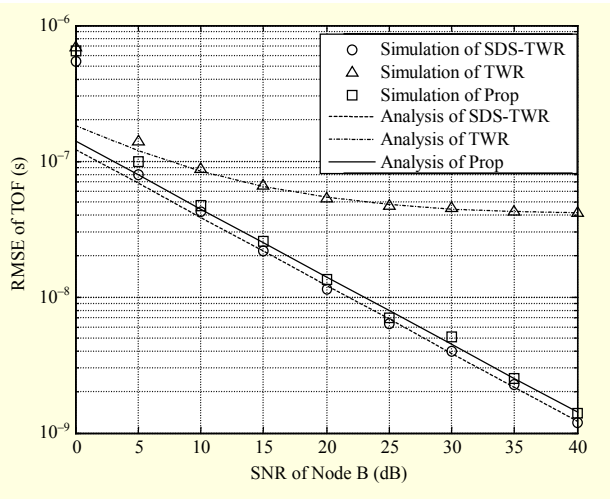

Fig. 8. Ranging performance of each protocol (frequency offset of Node A = 80 ppm; frequency offset of Node B = –80 ppm).

TOA estimation errors only. Thus, ranging accuracy increases as the SNR increases, as shown in Fig. 6. However, when there is a certain frequency offset, the estimation bias, not caused by noise but the offset, can saturate the RMSE curve of TWR, as shown in Figs. 7 and 8. In the cases of SDS-TWR and our proposed TWR, the bias caused by the frequency offset is quite small compared to the TOA estimation error due to noise under an SNR of 40 dB. From the simulation results, it is observed that our proposed TWR achieves almost the same ranging performance as that of SDS-TWR for a given frequency offset. Although SDS-TWR results in better performance than our proposed TWR, this is due to the TOA estimation error being reduced by TOF averaging.

VII. Conclusion

In this paper, a packet-reduced ranging method with an SR TOA estimation algorithm for chirp-based RTLS was presented. Our proposed ranging protocol using only two ranging packets achieved almost the same tolerance to the frequency offset as SDS-TWR. This approach reduces power consumption and ranging time. We analyzed the RMSE performance of our proposed ranging algorithm and compared it with that of the others, such as TWR and SDS-TWR, through computer simulations. We found that our proposed TWR prolongs the battery lifetime of RTLS nodes while keeping the ranging accuracy high.

References

[1] *IEEE Std. 802.15.4a-2007*, Aug. 2007, pp. 1-203.

[2] *ISO/IEC Std.* 24730-5, Mar. 2010, pp. 1-72.

[3] R. Hach, "Symmetric Double Sided – Two Way Ranging," contribution 802.15-05-0334-00-004a to the IEEE 802.15.4a Ranging Subcommittee, June 2005.

[4] Y. Jiang and V.C.M. Leung, "An Asymmetric Double Sided Two-Way Ranging for Crystal Offset," *Proc. Int. Symp. Signals, Syst. Electron. (ISSSE)*, Montreal, Québec, Canada, July 2007, pp. 525-528.

[5] M. Kwak and J. Chong, "A New Double Two-Way Ranging Algorithm for Ranging System," *2nd IEEE Int. Conf. Netw. Infrastructure Dig. Content*, Sept. 2010, pp. 470-473.

[6] H. Kim, "Double-Sided Two-Way Ranging Algorithm to Reduce Ranging Time," *IEEE Commun. Lett.*, vol. 13, no. 7, July 2009, pp. 486-488.

[7] S.F. Yau and Y. Bresler, "A Compact Cramer-Rao Bound Expression for Parametric Estimation of Superimposed Signals," *IEEE Trans. Signal Process.*, vol. 40, no. 5, May 1992, pp. 1226-1230.

[8] X. Li and K. Pahlavan, "Super-Resolution TOA Estimation with Diversity for Indoor Geolocation," *IEEE Trans. Wireless Comm.*, vol. 3, no. 1, Jan. 2004, pp. 224-234.

[9] P. Chevalier, A. Ferreol, and L. Albera, "High-Resolution Direction Finding From Higher Order Statistics: The 2q-MUSIC Algorithm," *IEEE Trans. Signal Process.*, vol. 54, no. 8, Aug. 2006, pp. 2986-2997.

[10] A.J. Vanderveen, M.C. Vanderveen, and A. Paulraj, "Joint Angle and Delay Estimation Using Shift-Invariance Techniques," *IEEE Trans. Sig. Proc.*, vol. 46, no. 2, Feb. 1998, pp. 405-418.

[11] S. Marcos, A. Marsal, and M. Benidir, "The Propagator Method for Source Bearing Estimation," *Signal Process.*, vol. 42, no. 2, 1995, pp. 121-138.

[12] S. Boumard and A. Mammela, "Robust and Accurate Frequency and Timing Synchronization Using Chirp Signals," *IEEE Trans. Broadcasting,* vol. 55, no. 1, Mar. 2009, pp. 115-123.

[13] S. Jang et al., "Robust and Accurate Packet Detection and Frequency Offset Compensation for CSS System," *3rd Int. Conf. Mobile Ubiquitous Computing Syst., Services Technol.*, Oct. 2009, pp. 169-172.

[14] D. Oh, S. Yoon, and J. Chong, "A Novel Time Delay Estimation Using Chirp Signals Robust to Sampling Frequency Offset for a Ranging System," *IEEE Comm. Lett.*, vol. 14, no. 5, May 2010, pp. 450-452.

[15] M. Oh, J. Kim, and H. Lee, "Traffic-Reduced Precise Ranging Protocol for Asynchronous UWB Positioning Networks," *IEEE Commun. Lett.*, vol. 14, no. 5, May 2010, pp. 432-434.

[16] L.J. Xing, L. Zhiwei, and F.C.P. Shin, "Symmetric Double Side Two Way Ranging with Unequal Reply Time," *Proc. 66th IEEE Veh. Technol. Conf. (VTC)*, Sept. 2007, pp. 1980-1983.

[17] Y.T. Chan and K.C. Ho, "Joint Time-Scale and TDOA Estimation: Analysis and Fast Approximation," *IEEE Trans. Signal Process.*, vol. 53, no. 8, Aug. 2005, pp. 2625-2634.

[18] D. Shin and T. Sung, "Comparisons of Error Characteristics between TOA and TDOA Positioning," *IEEE Trans. Aerospace Electr. Syst.*, vol. 38, no. 1, Jan. 2002, pp. 307-311.

[19] S.H. Song and Q.T. Zhang, "Multi-Dimensional Detector for UWB Ranging Systems in Dense Multipath Environments," *IEEE Trans. Wireless Commun.*, vol. 7, no. 1, Jan. 2008, pp. 175-183.

[20] J. Lee and S. Yoo, "Large Error Performance of UWB Ranging in Multipath and Multiuser Environments," *IEEE Trans. Microw. Theory Tech.*, vol. 54, no. 4, June 2006, pp. 1887-1895.

[21] N. Jeon et al., "Superresolution TOA Estimation With Computational Load Reduction," *IEEE Trans. Veh. Technol.*, vol. 59, no. 8, Oct. 2010, pp. 4139-4144.

[22] F. Ge et al., "Super-Resolution Time Delay Estimation in Multipath Environments," *IEEE Trans. Circuits Syst. I: Regular Papers*, vol. 54, no. 9, Sept. 2007, pp. 1977-1986.

[23] F. Li, R.J. Vaccaro, and D.W. Tufts, "Performance Analysis of the State-Space Realization (TAM) and ESPRIT Algorithms for DOA Estimation," *IEEE Trans. Antenna Propag.*, vol. 39, no. 3, Mar. 1991, pp. 418-423.

Daegun Oh received his BS, MS, and PhD in electronics engineering from Hanyang University, Seoul, Rep. of Korea, in 2005, 2007, and 2010, respectively. Currently, he is working at Daegu Gyeongbuk Institute of Science & Technology as a senior researcher. His current research interests include high resolution ranging algorithm development, modem design for the IEEE 802.15.4a chirp spread spectrum, superresolution algorithm development, and SoC design for imaging radar systems.

Seungryeol Go received his BS and MS in electronics and computer engineering from Hanyang University, Seoul, Rep. of Korea, in 2011, and 2013, respectively. Currently, he is working toward his PhD with the Department of Electronics and Computer Engineering, Hanyang University. His current research interests include indoor wireless communication SoC design for ranging and positioning, location estimation algorithms, two-way ranging protocol, and timing and frequency synchronization of chirp signals.

Jong-wha Chong received his BS and MS in electronics engineering from Hanyang University, Seoul, Rep. of Korea, in 1975 and 1979, respectively, and his PhD in electronics and communication engineering from Waseda University, Tokyo, Japan, in 1981. Since 1981, he has been a professor of the Department of Electronics Engineering, Hanyang University. From 1979 to 1980, he was a researcher in the C&C Research Center of Nippon Electronic Company. From 1983 to 1984, he was a visiting researcher in the Korean Institute of Electronics & Technology. In 1986 and 2008, he was a visiting professor at the University of California, Berkeley, CA, USA. He was the chairman of CAD & VLSI society in 1993 at the Institute of Electronics Engineers of Korea. He was the president of IEEK in 2007 and the president of KIEEE from 2009 to 2010. He is currently the chairman of Fusion SoC Forum. His current research interests are in SoC design methodology, including memory centric design and physical design automation of 3D-IC, indoor wireless communication SoC design for ranging and location, video systems, and power IT systems.